

Static and Dynamic Behaviors of Plasma Detachment in Divertor Simulator NAGDIS-II

S. Takamura¹⁾, N. Ohno¹⁾, Y. Uesugi¹⁾, D. Nishijima¹⁾, M. Motoyama¹⁾, N. Hattori¹⁾, H. Arakawa¹⁾,
N. Ezumi²⁾, S. Krasheninnikov³⁾, A. Pigarov³⁾, U. Wenzel⁴⁾

1) Department of Energy Engineering and Science, Graduate School of Engineering, Nagoya,
University, Nagoya 464-8603, Japan

2) Nagano National College of Technology, Nagano 381-8550, Japan

3) University of California at San Diego, La Jolla, California 92093-0411, USA

4) Max-Planck-Institut für Plasmaphysik, EURATOM Association, D-1011 Berlin, Germany

e-mail: takamura@nuee.nagoya-u.ac.jp

Abstract. We have performed comprehensive investigation on the static and dynamic behaviors in detached recombining plasmas in the linear divertor plasma simulator, NAGDIS-II. For the stationary plasma detachment, the transition from electron-ion recombination (EIR) to molecular activated recombination (MAR) has been observed by injecting hydrogen gas to high density He plasmas. The particle loss rate due to MAR is found to be comparable to that of EIR. We have also performed experiments on injection of a plasma heat pulse produced by rf heating to the detached recombining He plasma to demonstrate the dynamic behavior of the volumetric plasma recombination. Negative spikes in Balmer series line emissions were observed similar to the so called negative ELM observed in tokamak divertors, which were analyzed with collisional-radiative model in detail. Rapid increase of the ion flux to the target plate was observed associated with the re-ionization of the highly excited atoms generated by EIR.

1. Introduction

The divertor plasma simulator NAGDIS-II was constructed at 1997 in order to investigate edge plasma physics in fusion research, which has been providing a lot of basic knowledge concerning the plasma detachment in terms of heat and particle control in the divertor of magnetic confinement fusion devices. In this paper, we would like to describe the physics on plasma detachment and the structure of detached plasma obtained in the experimental work associated by the analysis using numerical fluid simulation and atomic-molecular collisional radiative (CR) model.

For stationary detached plasma, molecular activated recombination (MAR) associated with vibrationally excited hydrogen molecule has been a strong impact on edge plasma physics related to plasma detachment because its rate coefficient was predicted to be large compared to EIR at relatively high electron temperature. The experimental evidence of MAR has been clearly obtained in the NAGDIS-II[1]. However, it is not clear how MAR affects on the formation of detached plasmas compared to EIR. We will report comprehensive studies on stationary detached plasma, showing the transition from EIR to MAR depending on the concentration of hydrogen molecule and plasma density. The second part is devoted to the dynamic behaviors of detached plasmas under the ELM-like heat pulse irradiation. It has been recognized that the ELMs associated by a good confinement at the edge may bring an enormous energy to the divertor target through SOL and detached plasma. The understanding of the transport of ELM energy is rather poor at the moment, which might make the estimation of deposited heat load on the target in ITER very ambiguous. The inverse ELM which has been observed in JET[2] and ASDEX-U[3] for D_α emissions was found here to have double minimum in time for the Balmer series emissions from low excited levels and strong reductions of spectra from highly excited levels, showing the transition from recombining to ionizing and again back to recombining.

2. Experimental Results and Discussions

The NAGDIS-II device has water-cooled vacuum chamber of 2.5 m in length and 0.18 m in diameter equipped with 21 solenoid magnetic coils. The neutral pressure in the plasma test region can be controlled from 1 mtorr to 30 mtorr to realize attached and detached plasmas by feeding a secondary gas and/or changing pumping speed of the turbo-molecular pump near the target plate. Fast scanning probes are equipped at $X = 0.25$ m (entrance), 1.06 m (upstream), 1.39 m (midstream) and 1.72 m (downstream) from the anode to measure the plasma parameters. Spectra of light emissions are detected in the upstream midstream and downstream.

2.1 MAR and EIR in Detached He Plasma with Hydrogen Gas Puffing

At first, we generated the He plasma at a discharge current $I_d = 80$ A without any secondary gas puff, where the electron density n_e and T_e at the entrance are $4.0 \times 10^{19} \text{ m}^{-3}$ and 8.5 eV, respectively. He neutral pressure is adjusted to be 6.5 mtorr by controlling the pumping speed of turbo-molecular pump near the target plate. At this pressure, plasma detachment just starts. When a small amount of hydrogen gas was introduced into the He plasma, coexistence of He and hydrogen Balmer series spectra indicating EIR root were clearly observed as shown in Fig. 1. We can distinguish up to $n' = 21$ for hydrogen Balmer series. When more hydrogen gas is introduced and the partial pressure of hydrogen gas exceeds a critical level, both continuum and series of line emissions disappear, that is, EIR does not occur at all in this plasma condition.

In order to quantify the threshold value for transition of EIR, the emission intensities of He ($2^3\text{P}-10^3\text{D}$) and H (2-10) lines were employed as a degree of the EIR. Figure 2 (a) shows the dependence of these emission intensities on the hydrogen gas flow rate F_{H_2} , where $n_e \sim 2.3 \times 10^{19} \text{ m}^{-3}$ and $T_e \sim 6.0$ eV at entrance are kept constant. It is found that the both intensities drop rapidly around $F_{\text{H}_2} \sim 23$ sccm, which means that EIR becomes very weak. On the other hand, the ratio between H (2-10) and $\text{H}\alpha$ (2-3) is slightly increased with F_{H_2} in a small range of F_{H_2} and suddenly drops around the same critical flow rate of 23 sccm, because the population density at $n' = 3$ is selectively increased due to MAR process[1]. Concerning the density threshold, we can also determine the threshold value by the knee as shown in Fig. 2(b). Figure 3 shows F_{H_2} dependence of ion saturation currents measured in downstream, normalized by those at entrance. Although EIR disappears at the critical F_{H_2} mentioned above, the normalized ion saturation currents are monotonically decreased with an increase in F_{H_2} . Moreover, it is found that lower entrance plasma density leads to larger reduction rate of the ion saturation current. This result means that the

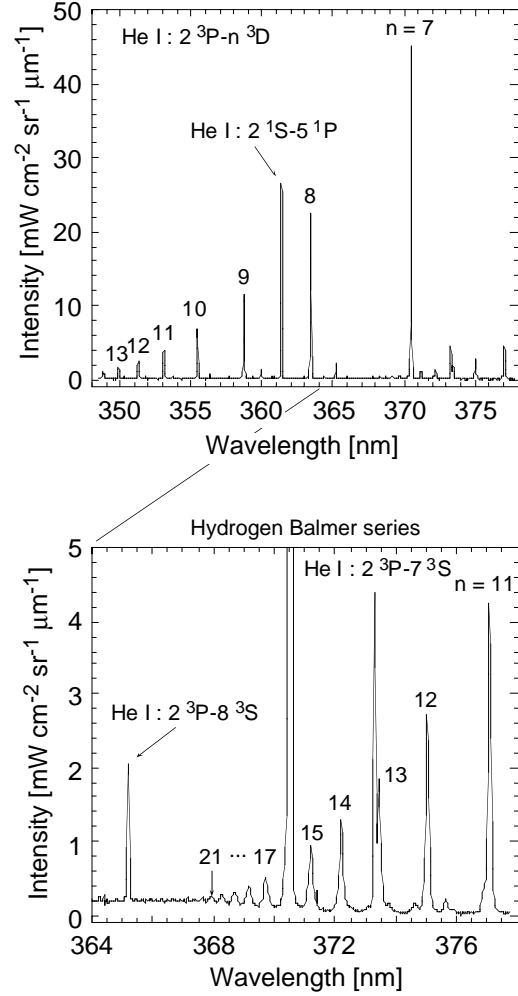


Fig. 1 Spectra from detached helium plasmas with small rate of hydrogen gas puff. The flow rate of hydrogen gas is 15 sccm. The plasma density at the entrance is $3.5 \times 10^{19} \text{ m}^{-3}$.

plasma particle loss due to MAR is getting larger with F_{H_2} and its loss rate is large enough to compensate that of EIR.

By using the threshold values determined in Fig. 2, we can illustrate the figure showing the parameter region at which EIR occurs. Figure 4 shows the boundary for EIR in the parameter space of n_e at entrance and F_{H_2} . It is found that a lower n_e at the entrance gives a lower threshold value F_{H_2} for EIR and vice versa. However, this boundary is not always correspondent to the threshold of MAR, because the ion flux in downstream is monotonically decreased with F_{H_2} as shown in Fig. 3. Therefore, more precisely, we need to say that hatched region shown in Fig. 4 means coexistence of EIR and MAR, and the another area is corresponding to the region where MAR is dominating. From these experimental results, we can conclude that the plasma volumetric recombination process coming from the effect of the molecular hydrogen (MAR) in our experimental environment exists with EIR and the plasma particle loss due to MAR is large enough to compensate that by EIR.

2. 2 Dynamic Behavior of Plasma Detachment during ELM-like Heat Pulse

Plasma heat pulse generated by the rf heating was introduced into detached He plasmas. The

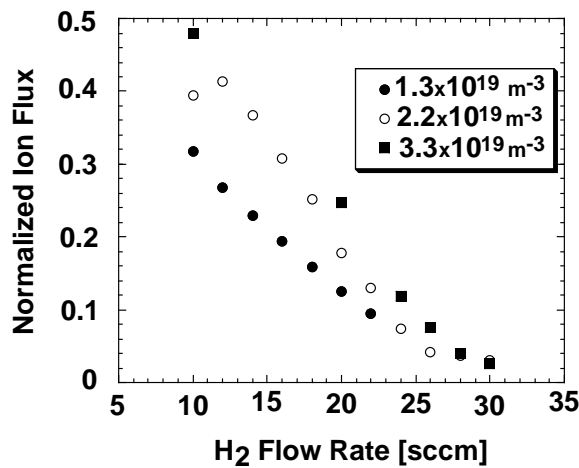


Fig. 3. Ion flux in downstream normalized by that at entrance as a function of hydrogen gas flow rate. Closed circles, open circles and closed squares are experimental data obtained at the plasma density of $1.3 \times 10^{19} \text{ m}^{-3}$, $2.2 \times 10^{19} \text{ m}^{-3}$, and $3.3 \times 10^{19} \text{ m}^{-3}$ at entrance, respectively.

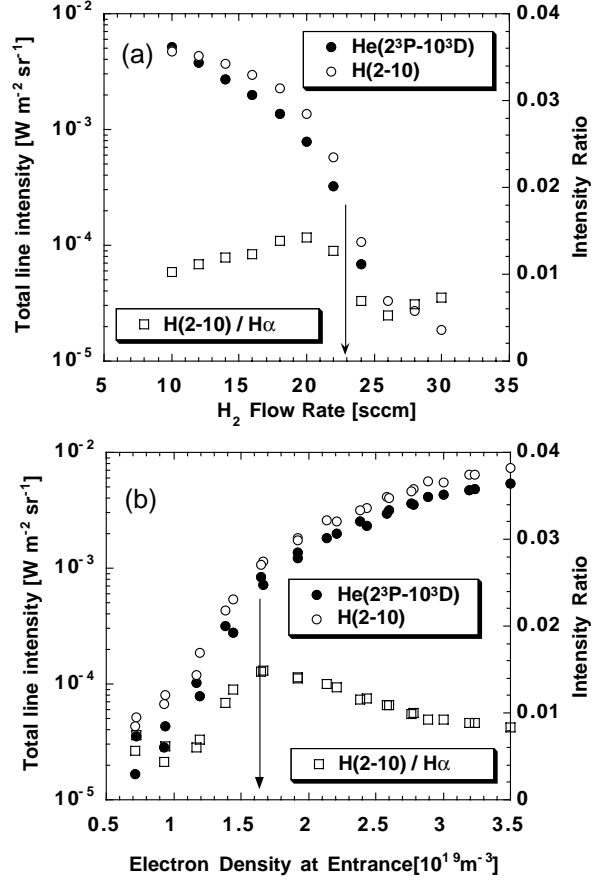


Fig. 2. Absolute line intensities of $\text{He}(2^3\text{P}-10^3\text{D})$ and $\text{H}(2-10)$ lines and intensity ratio of $\text{H}(2-10)$ and $\text{H}\alpha$ as functions of (a) hydrogen gas flow rate and (b) electron density at entrance.

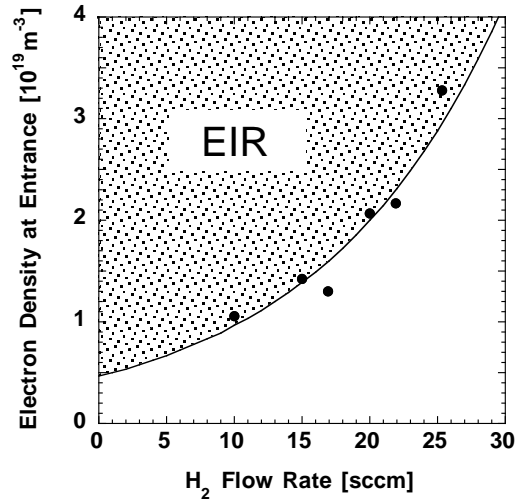


Fig. 4. Boundary for EIR in the parameter space of the hydrogen gas flow rate and electron density at entrance.

duration of the rf pulse is 0.05 msec. The rf power is 200 W. Figure 5 shows a typical time evolution of the line emission intensities from excited states (2^3P-n^3D) of He atom at the neutral He pressure of 9 mtorr. The electron temperature in the downstream is evaluated to be about 0.3 eV before the rf pulse is turned on. The line intensity of He (2^3P-3^3D) in the upstream, at which there is no recombining plasmas, is found to be increased by the electron impact excitation due to the energetic electrons generated by the rf heating. In the downstream, after the rf pulse is turned on, all line intensities are found to drop in time, which means that the EIR becomes weak. After the small first negative spikes appear around $t \sim 0.05$ msec, the emission intensities start to increase. They peak after the rf pulse is turned off, and gradually decrease. The second negative spikes clearly appear around $t \sim 0.2$ msec.

In order to quantitatively specify the characteristics of dynamic behaviors of He Balmer series emission, especially the negative spikes mentioned above, we have analyzed the emission intensities from the excited states of a He atom by using collisional-radiative (CR) model (Goto-Fujimoto code) including recombining as well as ionizing components. The population densities of the excited states of He atoms are thought to be governed by i) EIR and ii) electron impact excitation from the ground state. Figure 6 shows the dependence of emission intensity from $n' = 3$ on T_e as a parameter of n_e calculated with the CR model. It is proven that T_e^{eq} exists, at which the emission intensity is minimized. The reason is that in the low T_e region, lower T_e gives larger emission intensities because the population densities of the excited states are governed by EIR.

On the other hand, at the relatively high T_e , the emissions become large with the rise of T_e since the electron impact excitation is a dominating process. In short, the transition from the recombining phase to the ionizing phase and/or transition from the ionizing phase to the recombination phase give the negative spikes of emission intensities at T_e^{eq} .

Figure 7 shows the time evolution of the ion flux onto the target plate when the relatively large heat pulse was injected, where the duration of the pulse is 0.5 msec and the rf power is 1 kW. After the rf pulse is turned on, the ion flux is rapidly increased to be about 7 times larger than that before the rf pulse. It peaks around 0.03 msec and suddenly drops. On the other hand, the emission intensity of He (2^3P-5^3D) line becomes weak gradually after the start of rf pulse and starts to increase at 0.06 msec. Immediately after 0.1 msec, the time evolution of the ion flux and

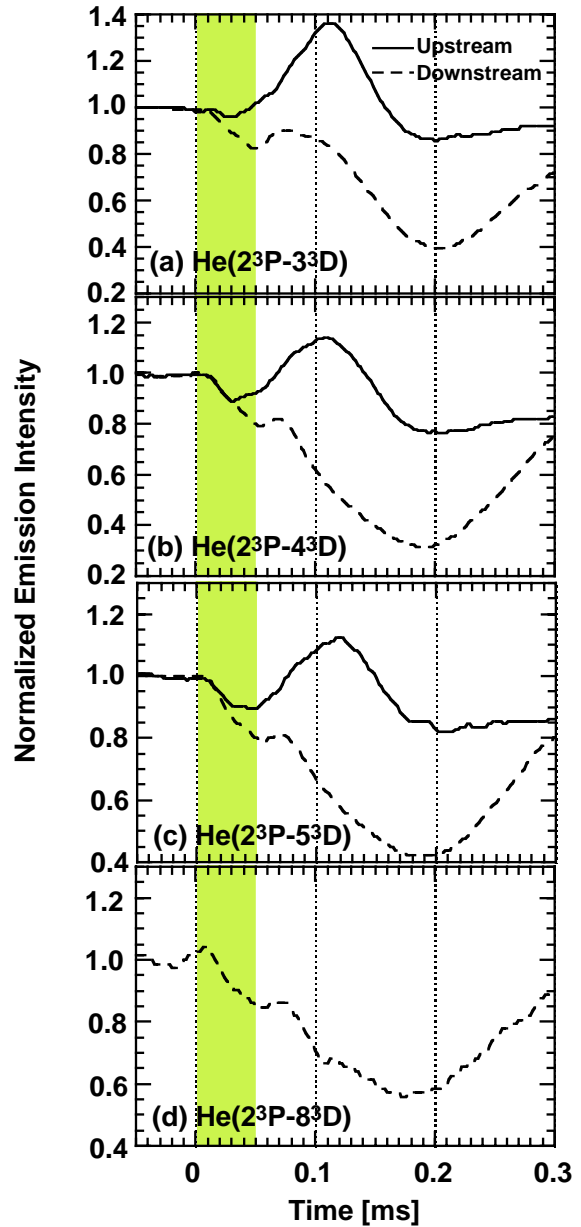


Fig. 5. Time evolution of emission intensities from detached helium plasmas observed in upstream and downstream at neutral pressure of 9 mtorr. The duration time of heat pulse is 0.05 msec and the rf power is 200 W.

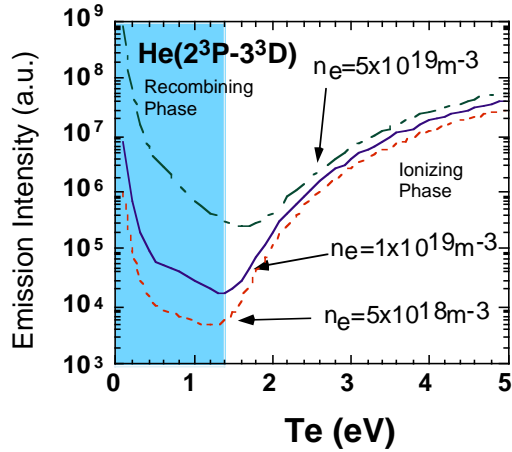


Fig. 6. Dependence of line emission intensities from principal quantum number $n' = 3$ on T_e calculated by collisional radiative model as a parameter of electron density.

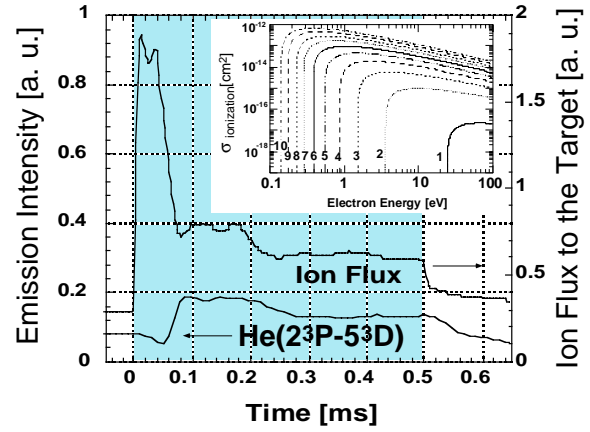


Fig. 7. Time evolution of ion flux onto the target plate and the line emission of He (2^3P-5^3D) from detached helium plasmas observed in downstream at a neutral pressure of 7.5 mtorr.

the emission intensity show almost the same tendency, which means that the electron impact excitation and ionization from the ground state are enhanced due to the energetic electrons generated by the rf heating to increase the ion flux and the emission intensity. On the other hand, the rapid increase of the ion flux at the beginning of the rf pulse can not be explained by the electron impact excitation from the ground state. Possible explanation is that highly excited atoms produced by EIR process are ionized by the energetic electrons, resulting in a decrease of the population densities of excited levels. The inset of Fig. 7 shows dependence of the ionization cross section on the electron energy, calculated by the Lotz formula. For He atoms in highly excited levels, the ionization cross section is found to be quite large. This calculation suggests that re-ionization of highly excited atoms due to the energetic electrons is playing an important role in the net recombination, which could be related to the rapid increase of the ion flux to the target plate and negative spike in the emission intensity of He (2^3P-5^3D).

3. Conclusion

We have performed comprehensive investigation on the static and dynamic behaviors in detached recombining plasmas in the linear divertor plasma simulator, NAGDIS-II. For the stationary plasma detachment, contributions of MAR and EIR to the plasma detachment have been investigated in detail to show the boundary for EIR observed for the electron density and hydrogen gas flow rate. The dynamic behaviors of detached recombining plasmas under the ELM-like heat pulse irradiation have also been studied. Negative spikes in Balmer series line emissions were clearly observed, which were analyzed with collisional-radiative model. Moreover, a strong enhancement of the ion flux to the target plate was observed by introducing the heat pulse, which can be explained by the re-ionization of the highly excited atoms generated by EIR process.

Reference

- [1] N. Ohno, N. Ezumi, S. Takamura et al., Phys. Rev. Lett. **81** (1998) 818.
- [2] A. Loarte et al., Nucl. Fusion **38** (1998) 331.
- [3] U. Wenzel et al., J. Nucl. Mater., **266-269** (1999) 1252.